



Reactivity of 3-hydroxy-3-methyl-2-butanone: Photolysis and reaction kinetics

H. Bouzidi, H. Laversin, A. Tomas, P. Coddeville, C. Fittschen, Gisèle El Dib,
E. Roth, A. Chakir

► To cite this version:

H. Bouzidi, H. Laversin, A. Tomas, P. Coddeville, C. Fittschen, et al.. Reactivity of 3-hydroxy-3-methyl-2-butanone: Photolysis and reaction kinetics. Atmospheric environment, 2014, 98, pp.540 - 548. 10.1016/j.atmosenv.2014.09.033 . hal-01072749

HAL Id: hal-01072749

<https://hal.science/hal-01072749>

Submitted on 8 Oct 2014

HAL is a multi-disciplinary open access archive for the deposit and dissemination of scientific research documents, whether they are published or not. The documents may come from teaching and research institutions in France or abroad, or from public or private research centers.

L'archive ouverte pluridisciplinaire **HAL**, est destinée au dépôt et à la diffusion de documents scientifiques de niveau recherche, publiés ou non, émanant des établissements d'enseignement et de recherche français ou étrangers, des laboratoires publics ou privés.

Reactivity of 3-hydroxy-3-methyl-2-butanone: Photolysis and OH reaction kinetics

H. Bouzidi¹, H. Laversin², A. Tomas^{1*}, P. Coddeville¹, C. Fittschen³, G. El Dib⁴,
E. Roth², A. Chakir²

¹Mines Douai, Département S.A.G.E, 59508 Douai, France

²Groupe de Spectrométrie Moléculaire et Atmosphérique, UMR CNRS 7331, Université de Reims, 51687 Reims, France

³Physico-chimie des Processus de Combustion et de l'Atmosphère, UMR CNRS 8522, Université Lille 1, 59655 Villeneuve d'Ascq, France

⁴Institut de Physique, Département de Physique Moléculaire, UMR 6251 CNRS, 35042 Rennes, France

* Corresponding author:

Alexandre TOMAS, alexandre.tomas@mines-douai.fr

Tel.: 33 327 712 651

Fax: 33 327 712 914

Manuscript prepared for submission to Atmospheric Environment

Abstract

Hydroxycarbonyl compounds are important secondary reaction products in the oxidation of Volatile Organic Compounds (VOCs) in the atmosphere. The atmospheric fate of these oxygenated VOCs is however poorly understood, especially the relevance of the photolytic pathway. In this work, a combined investigation of the photolysis and temperature-dependent OH radical reaction of 3-hydroxy-3-methyl-2-butanone (3H3M2B) is presented. A photolysis lifetime of about 4-5 days was estimated with a global quantum yield of 0.10. The OH reaction rate coefficient follows the Arrhenius trend (298 – 356 K) and could be modelled through the following expression: $k_{3H3M2B}(T) = (5.12 \pm 0.07) \times 10^{-12} \exp(-563 \pm 119/T)$ in $\text{cm}^3 \text{molecule}^{-1} \text{s}^{-1}$. A 3H3M2B atmospheric lifetime of 15 days towards the OH radical was evaluated. Our results showed that the photolysis pathway is the major degradation channel for 3H3M2B. Photolysis products were identified and quantified in the present work with a carbon balance of around 80% enabling a reaction mechanism to be proposed. The present work underlines the need for further studies on the atmospheric chemistry of oxygenated VOCs.

Keywords: 3-hydroxy-3-methyl-2-butanone, photolysis, kinetics, OH radicals, tropospheric lifetimes

1. Introduction

Oxygenated Volatile Organic Compounds (OVOCs) are critical components in the chemistry of the troposphere. These species constitute a large family of Volatile Organic Compounds (VOCs) (Atkinson et al., 2003) emitted from various anthropogenic and biogenic sources. More importantly, they are formed *in situ* as intermediates of photooxidation of several VOCs. Though scarce measurement data exist on the concentrations of multi oxygenated VOCs (e.g. (Matsunaga et al., 2000; Destailats et al., 2002; Spaulding et al., 2002)), evidence has been gained in the last decade for a significant role played by such compounds in atmospheric chemistry (Singh et al., 2001).

Chemical mechanism modelling studies indicate that more and more oxidized species are formed in the course of VOC oxidation, especially compounds bearing hydroxyl and carbonyl functions (Aumont et al., 2005; Madronich, 2006; Goldstein et al., 2007). Thus, β -hydroxycarbonyls can be formed from the OH^\bullet radical initiated reactions of diols with molar formation yields between 50% and 90% (Bethel et al., 2003), as well as from alcohols and alkenes (Tuazon et al., 1998; Reisen et al., 2003). In the atmosphere, OVOCs are supposed to react mainly with OH^\bullet radicals, although reactions with NO_3^\bullet , Cl and ozone cannot be excluded for some of the species in specific environments (Mellouki et al., 2003). The photolysis channel could be significant for carbonyl species (Moortgat, 2001; Bouzidi et al., 2014) and yet, its importance in the case of hydroxycarbonyl VOCs is almost unknown, while recent studies suggest that photolysis could be significant (Henry et al., 2012; Messaadia et al., 2012). Atmospheric chemistry of hydroxyacetone, the smallest hydroxyketone compound, is reasonably well understood (Orlando et al., 1999; Dillon et al., 2006). For larger hydroxycarbonyls ($\geq \text{C}_4$), degradation pathways have not been well characterized. The few available studies indicate that saturated hydroxyketones are mainly removed by OH^\bullet radicals (Aschmann et al., 2000; Magneron et al., 2003; Messaadia et al., 2012; El Dib et al., 2013; Messaadia et al., 2013; Sleiman et al., 2013). Reactivity with O_3 and NO_3^\bullet radicals is expected to be not important in the atmosphere (Calvert et al., 2011). Hydroxyketone lifetimes with respect to OH^\bullet radicals are in the range of about 1 day (e.g. for 4-hydroxy-2-butanone) to several days (e.g. 14 days for 3-hydroxy-3-methyl-2-butanone) (Aschmann et al., 2000; Calvert et al., 2011), thus showing large variability in the reactivity that can be attributed to the structure of the molecule. Recently, the determination of the absorption cross-sections for four hydroxycarbonyl ($\geq \text{C}_4$) compounds by (Messaadia et al., 2012) showed that all obtained spectra of these compounds were similar in shape with two absorption bands, the first one below 220 nm and the second one between 230 and 340 nm with a maximum in the wavelength range 265-290 nm. The tropospheric lifetime of 3H3M2B due to photolysis was estimated by Messaadia et al. (2012) to be at least 0.4 day using an upper limit of the photolysis rate assuming a quantum yield of unity. Therefore, atmospheric fate of these compounds may also be significantly affected by photolytic loss processes. As a consequence, a more detailed characterization of the photochemical fate of hydroxyketone compounds is clearly needed to make further progress in our understanding of the implication of these species in tropospheric chemistry and allow further extension of atmospheric chemistry models (especially for hydrocarbons) for improvement of air quality predictions.

The objective of the present work was to evaluate the importance of the photolysis and the OH -initiated reaction in the case of 3-hydroxy-3-methyl-2-butanone (3H3M2B), $((\text{CH}_3)_2\text{C}(\text{OH})\text{C}(\text{O})\text{CH}_3)$. This oxygenated VOC is an oxidation

product of the OH-initiated reaction of 2-methyl-2-butene (Tuazon et al., 1998). It has been observed in a measurement campaign carried out at San Francisco (Destailats et al., 2002). In the atmosphere, like other carbonyl compounds, 3H3M2B is expected to be removed by chemical reactions with the atmospheric photooxidants and by photolysis. The atmospheric degradation of this species is not well known however. In fact, only one kinetic study on the gas phase reaction of 3H3M2B is found in the literature (Aschmann et al., 2000a). In this study, the degradation of 3H3M2B due to its reaction with OH, NO₃ and O₃ was only investigated at room temperature and atmospheric pressure using a relative rate technique.

In order to elucidate the atmospheric fate of 3H3M2B, photolysis and kinetic studies as a function of temperature are necessary. In this work, photolysis of this species was studied from 270 to 390 nm and major products were analysed. Moreover, the OH-initiated reaction of 3H3M2B was studied and rate constants were determined as a function of temperature.

2. Experimental section

Experiments have been carried out using two different experimental set-ups, a simulation chamber made of Teflon film, located at the SAGE department of Mines Douai, and a temperature controlled Pyrex simulation chamber, located at University of Reims.

2.1 Photolysis study (Mines Douai)

2.1.1 Simulation chamber description and experimental conditions

The experimental procedure and equipments used for the photolysis experiments performed are briefly described in the following. More details on the experimental setup can be found in previous publications (Turpin et al., 2006; Szabo et al., 2009; Szabo et al., 2011). Experiments were carried out in a ~ 300 L FEP Teflon film chamber in an air-conditioned laboratory (296 K) and at 1 atm. Fluorescent tubes emitting in the 270-390 nm region with an energy peak at 312 nm were used for irradiation. In a typical experiment, a known amount of 3H3M2B was introduced in the chamber through a stream of purified air and the reaction mixture is allowed to stand for about 1 h in the dark. Three samples were then analysed to determine the initial concentration of the reactant. After the third sampling, the lamps are switched on and about 10 samples are taken along the photolysis experiments (lasting 6-8h) to monitor the concentrations of 3H3M2B and end-products over the time. 3H3M2B initial concentration was in the range of 9 to 50 ppm. Some experiments were conducted in the presence of excess cyclohexane (151-227 ppm), cyclopentane (280 ppm), m-xylene (33-280 ppm) or carbon monoxide (1330-3750 ppm) in order to scavenge any OH radicals formed in the reaction mechanism.

2.1.2 Test experiments

Test experiments were performed to investigate possible losses of 3H3M2B and products in the dark and during the photolysis experiments. First, deposition rates on the chamber walls were tested for by running experiments in the dark. Results showed that such losses were negligible for 3H3M2B, CH₂O, acetone, biacetyl, and methanol (rates < 1% per hour). In addition, tests for possible losses of products through photolysis were carried out. Results indicated that photolysis could be significant in the case of CH₂O, acetone and biacetyl with loss rates of 31%, 7% and 4% per hour, respectively. In the following, all the reported concentrations of CH₂O, acetone and biacetyl have been corrected for wall deposition and photolysis according to the rates determined in the test experiments. Formaldehyde was also corrected for production from acetone photolysis.

2.1.3 Sampling and analytical techniques

3H3M2B and photolysis product analysis were performed either by a ThermoDesorption-Gas phase Chromatograph (TD-GC) coupled with Fourier Transform Infrared (FTIR) spectroscopy and Flame Ionization Detection (FID) or by direct FTIR spectrometry using a White cell. The FTIR-White cell analytical system was similar to that used in the study carried out by (Bouzidi et al., 2014). The IR spectra typically result from the co-addition of 100 interferograms with a resolution of 2 cm^{-1} representing a measurement time of about 4 min. In the case of the TD-GC-FTIR-FID, gas samples of 100 cm^3 volume were collected every 45 min on Tenax adsorbent microtrap cooled down to -30°C . Injection was achieved by rapid heating of the microtrap to 300°C . Both analytical systems were connected to the chamber through a Teflon line heated to $\sim 338\text{ K}$. Some samples were also collected onto Tenax solid adsorbent and analysed by TD-GC-FID-Mass Spectrometry. Reactant and product concentrations were monitored using classical calibration procedures. Carbonyl products were analyzed following the same procedure as that described by (Bouzidi et al., 2014) using 2,4-dinitrophenylhydrazine (DNPH) derivatization followed by HPLC-UV analysis.

2.1.4 Actinometry

Acetone and acetaldehyde were used as actinometers in order to estimate the tropospheric photolysis lifetime and the effective quantum yields, as they have relatively similar UV absorption spectra compared to 3H3M2B (Messaadia et al., 2012). The photolysis frequencies of acetone and acetaldehyde in the simulation chamber in the presence of cyclopentane were $(0.070 \pm 0.01)\text{ h}^{-1}$ and $(0.22 \pm 0.02)\text{ h}^{-1}$, respectively. Acetone photolysis frequency calculated from the recommended values of cross-sections and quantum yields with a solar zenith angle of 20° within the lower troposphere for a cloudless day is about 0.00216 h^{-1} (Calvert et al., 2011). For acetaldehyde, a photolysis frequency of 0.0104 h^{-1} was measured at the Euphore chamber for a solar zenith angle of 20° (Calvert et al., 2011).

2.1.5 Chemicals

3H3M2B ($> 95\%$), 2,3-butanedione ($> 97\%$), cyclopentane ($> 99\%$), cyclohexane ($> 99\%$), m-xylène ($> 99\%$) and acetone ($> 99\%$) were purchased from Sigma-Aldrich, acetic acid ($> 99\%$) from Acros Organics and methanol from Fluka ($> 99\%$). Dry air was produced by a zero air generator (Claind AZ 2020). Carbon monoxide (4939 ppmv in N_2) was obtained from Praxair.

2.2 Oxidation by OH-radicals (GSMA-Reims)

2.2.1 Experimental set-up

The kinetics of the reaction of 3H3M2B with OH radicals was studied using a photo-chemical reactor coupled to a FTIR spectrometer. The set-up has been presented in details in a previous publication (Messaadia et al., 2013). Therefore, it will be described only briefly herein. The chamber is composed of a triple-jacket Pyrex cell (length of 2 m, internal diameter of 20 cm and total volume of 63 L). Multi-reflection was achieved through the use of gold-plated mirrors suitable for working with IR radiation, and was used to vary the path-length between 4 and 80 m. A primary pump was used to suck up the chamber to 10^{-3} mbar . The temperature in the chamber was regulated through the circulation of a thermostatic fluid (water or ethanol) between the inner and middle jackets. The fluid temperature and circulation were commanded by a Julabo FPW 90 thermostat. The working temperature range was from 298 K to 356 K. The temperature and the pressure in the chamber were respectively measured by a thermocouple and a MKS Baratron manometer with 0-1000 Torr full scale. 24 UV lamps emitting in the range of 300 to 400 nm were

symmetrically disposed around the chamber in order to ensure homogeneous photolysis and to generate OH-radicals from nitrous acid. The extremities of the chamber were sealed by inox plates which hold two optical windows made of ZnSe as well as the ports used for the introduction of the reacting species into the reaction medium.

An Equinox 55 FT-IR spectrometer provided by Bruker was used to monitor the concentration of the reactants and reference compounds inside the reaction medium. This FTIR spectrometer is equipped with a Globar IR source, a KBr beam-splitter, and two detectors (DTGS and MCT). Its operating spectral range varies between 600 and 4000 cm^{-1} , with a spectral resolution of 2 to 0.5 cm^{-1} . MCT was used as a detector in this study. The alignment of the IR beam inside the chamber was accomplished by using a He-Ne laser beam by adjusting the positions of the gold mirrors.

2.2.2 Experimental conditions

All experiments were performed in purified air. The OH reaction of 3H3M2B was studied relatively to tert-butyl alcohol (tert-C₄H₉OH) as a reference compound whose homogeneous reactivity towards OH-radicals is known. The OH radicals were generated by the photolysis of nitrous acid at 300-400 nm. Nitrous acid (HONO) was produced via the drop-wise addition of a 10 % sulphuric acid solution to a 0.2 M sodium nitrite solution. A flow of nitrogen gas was used to sweep along the generated acid into the chamber in the vapour phase. The used reagents were obtained from the following sources: Purified Air (99.999%) provided by Air Liquide, 3H3M2B (95%) provided by Sigma-Aldrich and tert-butyl alcohol (> 99.7%) provided by Fluka. They were further purified by repeated freeze-pump-thaw cycles before use.

Before starting the kinetic measurements, two tests were carried out: the first one aimed at evaluating the loss of 3H3M2B and the reference compound by photolysis in the absence of HONO. The second one consisted on monitoring the concentration of 3H3M2B and tert-C₄H₉OH in the absence of irradiations and in the presence of HONO to check for the stability of the reagents. These tests showed that photolysis and wall losses were negligible for both compounds. At each temperature, 2 to 3 independent experiments were carried out. Table 1 summarizes the experimental conditions.

The reference was chosen in such a way that at least one absorption band of the 3H3M2B does not exhibit any interference with those of the reference compound and vice versa, and that the OH-degradation rate constants of both, 3H3M2B and reference, are of the same order of magnitude. The rate constant of the reaction of tert-C₄H₉OH with OH used in this work is that reported by (Téton et al., 1996):

$$k_{\text{ref}} = (2.66 \pm 0.48) \times 10^{-12} \exp((-2240 \pm 1080)/RT) \text{ cm}^3 \text{ molecule}^{-1} \text{ s}^{-1} \quad (\text{I})$$

3. Results and discussion

3.1 Photolysis

3.1.1 Photolysis rate constants

The photolysis of 3H3M2B was carried out either in the absence or in the presence of excess of OH[•] radical scavenger. The photolysis rate constants $J_{3\text{H3M2B}}$ were determined by plotting the natural logarithm of the ratio $[3\text{H3M2B}]_0/[3\text{H3M2B}]_t$ versus time:

$$\ln \frac{[3\text{H3M2B}]_0}{[3\text{H3M2B}]_t} = J_{3\text{H3M2B}} \times t \quad (\text{II})$$

where $[3\text{H3M2B}]_0$ and $[3\text{H3M2B}]_t$ indicate the 3H3M2B concentrations at the initial and time t , respectively.

The 3H3M2B concentration data were well fitted to a straight line using a linear least-square procedure (Figure 1) and the slope of the linear regression (weighted by 1σ) represents $J_{3\text{H3M2B}}$. The experimental conditions and the photolysis frequencies obtained for 3H3M2B in the presence and absence of OH^\bullet scavenger are summarized in Table 2.

3H3M2B photolysis frequencies were found to be $(0.24 \pm 0.02) \text{ h}^{-1}$ and $(0.33 \pm 0.02) \text{ h}^{-1}$ in the presence and absence of OH^\bullet scavenger, respectively. The reported uncertainties represent one standard deviation of the slope of the regression line. In the absence of OH^\bullet scavenger, an increase of around 40% in $J_{3\text{H3M2B}}$ is noted. Using the average OH-radical rate constant obtained in the present work, $k_{\text{OH}+3\text{H3M2B}} = 7.6 \times 10^{-13} \text{ cm}^3 \text{ molecule}^{-1} \text{ s}^{-1}$ (see below) enables to estimate an OH^\bullet photostationary concentration of around $3 \times 10^7 \text{ radical cm}^{-3}$ from the observed difference in the photolysis frequencies. This suggests that OH^\bullet radicals were produced in the chemical mechanism, which is confirmed by the observation of cyclopentanol and cyclopentanone ($\text{OH}^\bullet + \text{cyclopentane}$ reaction products) in the presence of excess cyclopentane, or cyclohexanol and cyclohexanone ($\text{OH}^\bullet + \text{cyclohexane}$ reaction products) in the presence of cyclohexane.

3.1.2 Effective quantum yields

From the obtained photolysis frequencies, the effective quantum yield of the 3H3M2B photolysis can be calculated using acetone and acetaldehyde actinometry experiments according to the following equation (Bacher et al., 2001; Bouzidi et al., 2014):

$$\Phi_{3\text{H3M2B}} = \frac{J_{3\text{H3M2B}}/J_{\text{actin}}}{J_{3\text{H3M2B}}^{\text{calc}}/J_{\text{actin}}^{\text{calc}}} \quad (\text{III})$$

$J_{3\text{H3M2B}}^{\text{calc}}$ and $J_{\text{actin}}^{\text{calc}}$ are the 3H3M2B and actinometer (acetone or acetaldehyde) photolysis frequencies, respectively, calculated using:

$$J_{3\text{H3M2B}}^{\text{calc}} = \int_{\lambda} \Phi_{3\text{H3M2B}}(\lambda) \times \sigma_{3\text{H3M2B}}(\lambda) \times F(\lambda) d\lambda \quad (\text{IV})$$

$$\text{and } J_{\text{actin}}^{\text{calc}} = \int_{\lambda} \Phi_{\text{actin}}(\lambda) \times \sigma_{\text{actin}}(\lambda) \times F(\lambda) d\lambda \quad (\text{V})$$

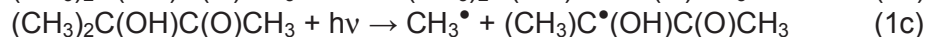
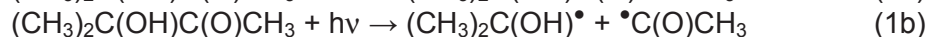
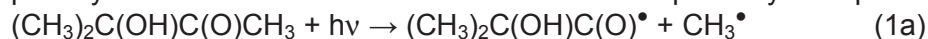
where $\Phi_{3\text{H3M2B}}(\lambda)$ and $\Phi_{\text{actin}}(\lambda)$ represent the 3H3M2B and actinometer wavelength-dependent quantum yields, respectively. $\sigma_{3\text{H3M2B}}(\lambda)$ and $\sigma_{\text{actin}}(\lambda)$ are the 3H3M2B and actinometer absorption cross-sections, respectively and $F(\lambda)$ the relative actinic flux intensity. For 3H3M2B, cross-sections were from (Messaadia et al., 2013) and quantum yields in Equation (IV) were set to unity. $\sigma_{\text{acetone}}(\lambda)$, $\Phi_{\text{acetone}}(\lambda)$, $\sigma_{\text{acetaldehyde}}(\lambda)$ and $\Phi_{\text{acetaldehyde}}(\lambda)$ were all from the last evaluation from IUPAC (IUPAC, 2013). Using Equation (III), the 3H3M2B effective quantum yields are: $\Phi_{3\text{H3M2B}} = 0.85 \pm 0.30$ with acetone as actinometer and $\Phi_{3\text{H3M2B}} = 0.76 \pm 0.20$ with acetaldehyde as actinometer. An average quantum yield of $\Phi_{3\text{H3M2B}} = 0.81 \pm 0.30$ is thus recommended over the wavelength range 270-390 nm.

The main sources of uncertainties are the 3H3M2B and actinometer absorption cross-sections, the acetone and acetaldehyde quantum yields and the measured 3H3M2B, acetone and acetaldehyde photolysis frequencies. Using the propagation of errors yields an overall uncertainty of 35% and 28% on the 3H3M2B quantum yields with acetone and acetaldehyde, respectively. The fairly large effective 3H3M2B quantum yields are comparable to those obtained for hydroxyacetone (Orlando et al., 1999): $\Phi_{\text{hydroxyacetone}} = 0.65 \pm 0.25$ for 240-420 nm

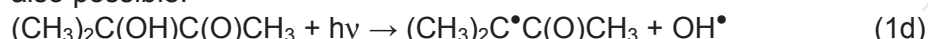
and $\Phi_{\text{hydroxyacetone}} < 0.6$ for $\lambda > 290$ nm. Note that these quantum yields values are the only data for hydroxyketone species known in the literature.

3.1.3 Photolysis products

Product analysis was carried out to unravel the mechanism of 3H3M2B photolysis. Three carbon-carbon bond dissociation pathways are possible:



In addition, the direct OH^\bullet release from the carbon – hydroxy group dissociation is also possible:

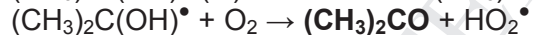
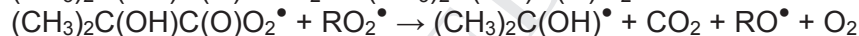
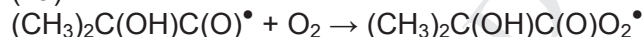


Five major reaction products – acetone, acetic acid, formaldehyde, CO and methanol – were observed. Figure 2 shows reactant and product time profiles obtained in the presence of m-xylene as OH-scavenger. The shape of the profiles for acetone, formaldehyde and methanol displays non-zero derivative at the origin, indicating that these compounds are primary products. On the contrary, carbon monoxide and acetic acid present secondary product profiles with a delay time before their concentrations increase.

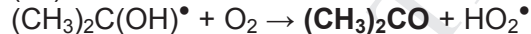
Yield plots in the form of [products] vs. $[\text{3H3M2B}]_{\text{reacted}}$ are shown in Figure 3 for the primary products: linear profiles were obtained for acetone and formaldehyde while a slightly increasing curved profile was obtained for methanol. Table 2 summarizes the corresponding corrected yields obtained in the photolysis of 3H3M2B with and without OH^\bullet scavenger.

Acetone $(\text{CH}_3)_2\text{CO}$ is expected to originate from channels (1a), (1b) and/or (1d) through the following reaction sequences (where RO_2^\bullet represents a peroxy radical):

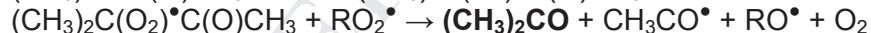
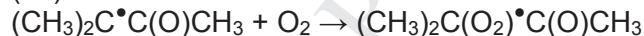
(1a)



(1b)



(1d)



As an acetone yield of nearly 1 is obtained, it is concluded that the branching to channel (1c) (which is not supposed to yield acetone) is rather low ($< 2\%$).

Formaldehyde arises from the radical recombination of $\text{CH}_3\text{O}_2^\bullet$: for example, the $\text{CH}_3\text{O}_2^\bullet$ self reaction leads to CH_2O :



with a branching ratio $k_{2b}/k_2 = 0.63$ recommended by (Sander et al., 2011).

The CH_2O yield of 23% (corrected for wall loss, photolysis and production from acetone photolysis) - well below 100% - indicates that a fraction of the $\text{CH}_3\text{O}_2^\bullet$ radicals will react with HO_2^\bullet in a terminating channel to form essentially methylhydroperoxide (Orlando et al., 2012) and that some of the $\text{CH}_3\text{C}(\text{O})\text{O}_2^\bullet$ radicals will be lost through the $\text{CH}_3\text{C}(\text{O})\text{O}_2^\bullet + \text{HO}_2^\bullet$ reaction which gives only 0.44 $\text{CH}_3\text{O}_2^\bullet$ (Dillon et al., 2008). Note that this last reaction is known to produce OH radicals with branching ratios between 0.4 and 0.6 (Gross et al., 2014) and may represent the sole source of OH radicals in the 3H3M2B photolysis. Noteworthy the CH_2O yield

decreases from the conditions with OH-scavenger (23%) to the conditions without OH-scavenger (16%) probably due to the $\text{OH}^\bullet + \text{CH}_2\text{O}$ reaction.

Methanol mostly originates from the molecular channel of $\text{CH}_3\text{O}_2^\bullet$ peroxy radical reactions:

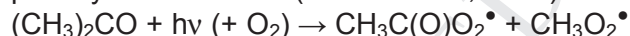


Results from experiments with m-xylene and CO as OH^\bullet scavenger showed a higher methanol yield with m-xylene (11%) than with CO (6%), revealing that the additional RO_2^\bullet radicals from m-xylene + OH^\bullet convert more $\text{CH}_3\text{O}_2^\bullet$ into CH_3OH (as CO + OH^\bullet leads to $\text{HO}_2^\bullet + \text{CO}_2$ and no RO_2^\bullet).

In addition to the three major primary products, carbon monoxide and acetic acid (AA) were also observed in the present study. The plots $[\text{CO}]$ and $[\text{AA}]$ vs. $[\text{3H3M2B}]_{\text{reacted}}$ are not linear but follow roughly a second order polynomial with a zero derivative at the origin, indicating the occurrence of only secondary sources both in presence and in absence of OH^\bullet scavenger (Figure 4). Direct formation of CO from 3H3M2B photolysis through $(\text{CH}_3)_2\text{C}(\text{OH})\text{C}(\text{O})\text{CH}_3 + h\nu \rightarrow (\text{CH}_3)_2\text{C}(\text{OH})^\bullet + \text{CO} + \text{CH}_3^\bullet$ is thus excluded. It should be stressed that a larger amount of CO is quantified in the absence of OH^\bullet scavenger. The secondary formation of CO may thus be attributed essentially to formaldehyde photolysis and reaction with OH^\bullet .

Similarly, the absence of acetic acid formation at the beginning of the reaction (Figure 4) suggests a unique secondary origin for this product. As AA is produced through $\text{CH}_3\text{C}(\text{O})\text{O}_2^\bullet + \text{HO}_2^\bullet/\text{RO}_2^\bullet$ reactions (Tomas et al., 2001; Sander et al., 2011), we conclude that the photodissociation channels (1b) and (1d) (both producing $\text{CH}_3\text{C}(\text{O})\text{O}_2^\bullet$) are minor channels. Assuming that AA only comes through the $\text{CH}_3\text{C}(\text{O})\text{O}_2^\bullet + \text{HO}_2^\bullet$ reaction with a branching ratio of 0.2 (Tomas et al., 2001) and using an AA detection limit of 50 ppb enable a rough estimation of the maximum branching ratio for the (1b) + (1d) channels of 5% to be calculated.

The secondary formation of acetic acid can be primarily attributed to the photolysis of acetone (Calvert et al., 2011):



followed by peroxy radical reactions of $\text{CH}_3\text{C}(\text{O})\text{O}_2^\bullet$ (Tomas et al., 2001). The heterogeneous formation of acetic acid in the $\text{OH}^\bullet + \text{acetone}$ reaction reported by (Turpin et al., 2006) is probably not significant in the present conditions, as more AA is observed when OH radicals are scavenged. We also suspect the $\text{OH}^\bullet + \text{m-xylene}$ reaction that produces methylglyoxal with yields of about 40% (Calvert et al., 2002). Methylglyoxal can readily be photolysed into $\text{CH}_3\text{CO}^\bullet + \text{HCO}^\bullet$, giving $\text{CH}_3\text{C}(\text{O})\text{O}_2^\bullet$, HO_2^\bullet and CO. This source could explain the large difference in the AA formed with m-xylene as OH-scavenger compared to that formed in the absence of OH-scavenger (see Figure 4). This result underlines the role that can be played by a scavenger in modifying the type and amount of peroxy radicals in the investigated chemical system, and thus the products observed.

Minor products were also identified: 2,3-butanedione (or biacetyl, $\text{CH}_3\text{C}(\text{O})\text{C}(\text{O})\text{CH}_3$), hydroxyacetone and methylglyoxal. Biacetyl yields of 1.4% and 0.4% have been quantified in the absence and presence of OH scavengers. This α -diketone is expected to originate from the photolysis channel (1c). The increase in the biacetyl yields between OH^\bullet and no OH^\bullet conditions may be attributed to a weak biacetyl formation through $\text{OH}^\bullet + \text{3H3M2B}$. Finally, hydroxyacetone and methylglyoxal were also tentatively identified and quantified with very low yields (< 0.5%).

Overall, the carbon balance obtained in the present work represents nearly 80%. The lacking products are assumed to be mainly peroxides formed by $\text{RO}_2^\bullet + \text{HO}_2^\bullet$ reactions (Orlando et al., 2012).

3.1.4 Mechanism interpretation

Based on the reaction product observations, it is possible to propose a simplified photolysis mechanism of 3H3M2B as shown in the scheme displayed in Figure 5. The high yields of acetone (98%) coupled with negligible amounts of CO and acetic acid at the beginning of the experiments in the presence of OH^\bullet scavenger indicates that the photolysis of 3H3M2B proceeds mainly through the rupture of the C1-C2 bond of the molecule (channel (1a)). Photolysis channels (1b) and (1d), both producing acetic acid, and channel (1c) leading to 2,3-butanedione, respectively, are of minor importance.

3.2 OH reaction kinetics

The kinetics of the reaction of OH radicals with 3H3M2B was determined relatively to that of a reference compound using the following equation:

$$\ln\left(\frac{[\text{3H3M2B}]_{t_0}}{[\text{3H3M2B}]_t}\right) = R \times \ln\left(\frac{[\text{ref}]_{t_0}}{[\text{ref}]_t}\right) \quad (\text{VI})$$

where $[\text{3H3M2B}]_{t_0}$ and $[\text{ref}]_{t_0}$ are the initial concentrations of 3H3M2B and tert-butyl alcohol at time t_0 , respectively; $[\text{3H3M2B}]_t$ and $[\text{ref}]_t$ are the concentrations of 3H3M2B and tert-butyl alcohol at time t , respectively and R is the ratio of rate constants ($R = k_{\text{3H3M2B}}/k_{\text{ref}}$) where k_{ref} is the rate constant of the reference reaction. A plot of $\ln([\text{3H3M2B}]_{t_0}/[\text{3H3M2B}]_t)$ as a function of $\ln([\text{ref}]_{t_0}/[\text{ref}]_t)$ results in a straight line with the slope equal to R . Knowing k_{ref} , it is possible to determine k_{3H3M2B} , the rate constant of the reaction of OH-radicals with 3H3M2B. During an experiment, IR spectra were recorded every 5 minutes. Each spectrum constitutes the average of 20 accumulated acquisitions leading to a signal to noise ratio of ~ 15 . The obtained data are presented in the form of $\ln([\text{3H3M2B}]_{t_0}/[\text{3H3M2B}]_t)$ vs. $\ln([\text{ref}]_{t_0}/[\text{ref}]_t)$. As can be seen on Figure 6, good linearity is observed with correlation coefficients greater than 0.91. The rate constants obtained in the present study are reported in Table 3. The given rates are derived from the average of 2 to 4 independent measurements. At 298 K, the average rate constant for the reaction of 3H3M2B with OH radicals is: $k_{\text{3H3M2B}} = (7.6 \pm 0.5) \times 10^{-13} \text{ cm}^3 \text{ molecule}^{-1} \text{ s}^{-1}$.

For each experiment, the overall error in the rate constant values reported in this work is calculated using propagation of error according to the following relation:

$$\Delta k_{\text{3H3M2B}} = k_{\text{3H3M2B}} \sqrt{(\Delta k_{\text{ref}}/k_{\text{ref}})^2 + (\Delta R/R)^2} \quad (\text{VII})$$

where k_{ref} , Δk_{ref} are the rate constant of the reference reaction and the uncertainty on this parameter, respectively and $R = k_{\text{3H3M2B}}/k_{\text{ref}}$ is the slope of the plot according to Equation (VI) with ΔR the uncertainty on this value. Errors originate mainly from:

- (i) the determination of k_{ref} : this error varies from 10% to 20% according to the temperature (Téton et al., 1996);
- (ii) the determination of the slope R : this parameter is determined directly from the experimental data. The uncertainty on this parameter is related to the areas corresponding to the absorption bands of 3H3M2B and the reference compound. The standard deviation in R values obtained for each set of experiments varies between 10% and 25% (Table 3), which indicates that the experiments are fairly reproducible.

The Arrhenius plot derived from the experimental rate constants (Table 3) is presented in Figure 7 and shows a good linearity. The corresponding Arrhenius equation is:

$$k_{3\text{H3M2B}}(T) = (5.12 \pm 0.07) \times 10^{-12} \exp(-563 \pm 119/T) \text{ cm}^3 \text{ molecule}^{-1} \text{ s}^{-1}$$

In contrast to other hydroxyketones studied in our laboratory (Messaadia et al., 2013), the rate constant $k_{3\text{H3M2B}}$ exhibits a slight positive temperature dependence. However, this temperature coefficient remains relatively weak (E/R around 600 K). This indicates that this reaction may proceed initially via the reversible formation of unstable intermediate complexes.

Until now, no kinetic data were reported in the literature for the reaction of 3H3M2B with OH radicals as a function of temperature. Only one study regarding the kinetics of OH-oxidation of 3H3M2B exists but only at room temperature (Aschmann et al., 2000). Our value of $(7.6 \pm 0.5) \times 10^{-13} \text{ cm}^3 \text{ molecule}^{-1} \text{ s}^{-1}$ is in good agreement with this determination (of $(9.4 \pm 3.7) \times 10^{-13} \text{ cm}^3 \text{ molecule}^{-1} \text{ s}^{-1}$) with a difference less than 20%.

It is also possible to compare the reactivity of 3H3M2B to that of other hydroxyketones for which the hydroxyl group is attached to the carbon atom located in the α position with respect to the carbonyl group, namely 1-hydroxy-2-butanone, 3-hydroxy-2-butanone and 4-hydroxy-3-hexanone. The kinetic rate constants of the gas-phase reaction of OH radicals with these compounds are ($\text{cm}^3 \text{ molecule}^{-1} \text{ s}^{-1}$): $(7.7 \pm 0.7) \times 10^{-12}$ (Aschmann et al., 2000), $(9.60 \pm 0.30) \times 10^{-12}$ (Messaadia et al., 2013) and $(15.1 \pm 3.1) \times 10^{-12}$ (Aschmann et al., 2000) for 1-hydroxy-2-butanone, 3-hydroxy-2-butanone and 4-hydroxy-3-hexanone, respectively. As expected, the reactivity of 3H3M2B towards OH radicals is lower than that of the other α -hydroxyketones by at least one order of magnitude. This lower reactivity can be attributed to the lack of secondary or tertiary H-atoms in the structure of the 3H3M2B molecule.

4. Atmospheric implications

The photolysis frequency of 3H3M2B determined in the present work is specific to the experimental setup used and cannot be directly applied for the estimation of the atmospheric lifetime. However, the 3H3M2B atmospheric photolysis frequency ($J_{3\text{H3M2B}}^{\text{atm}}$) can be estimated using the known photolysis frequencies of actinometers (acetone and acetaldehyde) in the troposphere ($J_{\text{actin}}^{\text{atm}}$) through the following equation:

$$J_{3\text{H3M2B}}^{\text{atm}} = J_{3\text{H3M2B}} \times \frac{J_{\text{actin}}^{\text{atm}}}{J_{\text{actin}}} \quad (\text{VIII})$$

Taking into account the experimental photolysis rate constants of 3H3M2B $J_{3\text{H3M2B}}$ and actinometer J_{actin} measured in the reaction chamber allows to estimate an average photolysis frequency of 3H3M2B in the troposphere of $J_{3\text{H3M2B}}^{\text{atm}} = 0.0095 \text{ h}^{-1}$. A global uncertainty of about 70% is associated with $J_{3\text{H3M2B}}^{\text{atm}}$ principally due to the uncertainties on J_{actin} of at least 50% (Calvert et al., 2011). Furthermore, using the absorption cross sections of 3H3M2B (Messaadia et al., 2012) and the actinic flux at 40°N, 1st July and 20° zenithal angle enables calculating an upper limit of the 3H3M2B photolysis frequency $J_{3\text{H3M2B},\text{max}}$ of 0.094 h^{-1} in the atmosphere (assuming a 3H3M2B quantum yield of 1 over the whole absorption range). Finally, comparing the estimated and maximum $J_{3\text{H3M2B}}$ values yields an effective quantum yield of $\Phi = J_{3\text{H3M2B}}^{\text{atm}} / J_{3\text{H3M2B},\text{max}} = 0.0095 / 0.094 \approx 0.10$ for 3H3M2B in the atmosphere with around 80% combined uncertainty.

Data on atmospheric photolysis frequencies of hydroxyketones are very scarce in the literature. The estimated photolysis frequency of 3H3M2B in the troposphere is roughly a factor two higher than the J value for hydroxyacetone (HA): $J_{HA}^{atm} \approx (0.0054 \pm 0.0018) \text{ h}^{-1}$ while a factor two lower than the higher limit determined for 4-hydroxy-4-methyl-2-pentanone (4H4M2P) $J_{4H4M2P}^{atm} \leq 0.018 \text{ h}^{-1}$ (Calvert et al., 2011). The atmospheric lifetime of 3H3M2B can then be calculated according to:

$$\tau_{3H3M2B}^{atm} = \frac{1}{J_{3H3M2B}^{atm}} \quad (IX)$$

The calculated lifetime of 3H3M2B with respect to photolysis is about 4 - 5 days. An atmospheric lifetime of 15 days due to reaction with OH^\bullet radicals is estimated according to the equation $\tau = 1/k_{3H3M2B} \times [\text{OH}^\bullet]$ by using a 24 h daytime average global tropospheric OH^\bullet concentration of $1 \times 10^6 \text{ molecule cm}^{-3}$ (Atkinson et al., 1997). Thus, it is clear that photolysis is the major oxidation pathway for 3H3M2B in the gas-phase. It should be noted that other heterogeneous loss processes for 3H3M2B including physical processes (dry deposition) and uptake by clouds followed by wet deposition may be important. Regional impacts should thus be expected for 3H3M2B: photolysis of 3H3M2B represents a source of acetone and formaldehyde, affecting the atmospheric oxidative capacity and the tropospheric ozone budget.

The data obtained in this work suggest that the reactivity of hydroxycarbonyls may be very sensitive to their chemical structures. While the OH^\bullet reaction is generally the major tropospheric loss process for hydroxycarbonyls, the absence of H-atom in the β position to the carbonyl group of 3H3M2B strongly depletes its reactivity towards OH^\bullet radicals and consequently enhances the importance of the photolysis channel in the atmosphere.

Aknowledgements

The authors gratefully thank the INSU-LEFE French programme. SAGE laboratory participates in the Institut de Recherche en ENvironnement Industriel (IRENI), which is financed by the Communauté Urbaine de Dunkerque, the Nord-Pas de Calais Regional Council, the French Ministry of Higher Education and Research, the CNRS and the European Regional Development Fund. The present work also takes place in the Labex CaPPA (Chemical and Physical Properties of the Atmosphere, ANR-11-LabEx-0005-01) supported by the French research agency ANR. H. Bouzidi is grateful for a PhD scholarship from the Nord-Pas de Calais Regional Council and Mines Douai.

References

- Aschmann S. M., Arey J., Atkinson R. (2000). Atmospheric chemistry of selected hydroxycarbonyls. *Journal of Physical Chemistry A* 104, 3998-4003.
- Atkinson R., Arey J. (2003). Gas-phase tropospheric chemistry of biogenic volatile organic compounds: a review. *Atmospheric Environment* 37, S197-S219.
- Atkinson R., Baulch D. L., Cox R. A., Hampson R. F., Kerr J. A., Rossi M. J., Troe J. (1997). Evaluated Kinetic and Photochemical Data for Atmospheric Chemistry: Supplement VI. IUPAC Subcommittee on Gas Kinetic Data Evaluation for Atmospheric Chemistry. *Journal of Physical and Chemical Reference Data* 26, 1329-1499.
- Aumont B., Szopa S., Madronich S. (2005). Modelling the evolution of organic carbon during its gas-phase tropospheric oxidation: development of an explicit model

- based on a self generating approach. *Atmospheric Chemistry and Physics* 5, 2497-2517.
- Bacher C., Tyndall G. S., Orlando J. J. (2001). The atmospheric chemistry of glycolaldehyde. *Journal of Atmospheric Chemistry* 39, 171-189.
- Bethel H. L., Atkinson R., Arey J. (2003). Hydroxycarbonyl Products of the Reactions of Selected Diols with the OH Radical. *The Journal of Physical Chemistry A* 107, 6200-6205.
- Bouzidi H., Fittschen C., Coddeville P., Tomas A. (2014). Photolysis of 2,3-pentanedione and 2,3-hexanedione: kinetics, quantum yields, and product study in a simulation chamber. *Atmospheric Environment* 82, 250-257.
- Calvert J. G., Atkinson R., Becker K. H., Kamens R. M., Seinfeld J. H., Wallington T. J., Yarwood G. (2002). The mechanisms of atmospheric oxidation of aromatic hydrocarbons. New York, Oxford University Press.
- Calvert J. G., Mellouki A., Orlando J. J., Pilling M. J., Wallington T. J. (2011). The mechanisms of atmospheric oxidation of the oxygenates. New York, Oxford University Press.
- Destailats H., Spaulding R. S., Charles M. J. (2002). Ambient Air Measurement of Acrolein and Other Carbonyls at the Oakland-San Francisco Bay Bridge Toll Plaza. *Environmental Science & Technology* 36, 2227-2235.
- Dillon T. J., Crowley J. N. (2008). Direct detection of OH formation in the reactions of HO₂ with CH₃C(O)O₂ and other substituted peroxy radicals. *Atmospheric Chemistry and Physics* 8, 4877-4889.
- Dillon T. J., Horowitz A., Hölscher D., Crowley J. N., Vereecken L., Peeters J. (2006). Reaction of HO with hydroxyacetone (HOCH₂C(O)CH₃): rate coefficients (233–363 K) and mechanism. *Physical Chemistry Chemical Physics* 8, 236–246.
- El Dib G., Sleiman C., Canosa A., Travers D., Courbe J., Sawaya T., Mokbel I., Chakir A. (2013). First experimental determination of the absolute gas-phase rate coefficient for the reaction of OH with 4-hydroxy-2-butanone (4H2B) at 294 K by vapor pressure measurements of 4H2B. *Journal of Physical Chemistry A* 117, 117-125.
- Goldstein A. H., Galbally I. E. (2007). Known and unexplored organic constituents in the Earth's atmosphere. *Environmental Science and Technology* March 1, 1515-1521.
- Gross C. B. M., Dillon T. J., Schuster G., Lelieveld J., Crowley J. N. (2014). Direct kinetic study of OH and O₃ formation in the reaction of CH₃C(O)O₂ with HO₂. *Journal of Physical Chemistry A* 118, 974–985.
- Henry K. M., Donahue N. M. (2012). Photochemical aging of α-pinene secondary organic aerosol: Effects of OH radical sources and photolysis. *Journal of Physical Chemistry A* 116, 5932-5940.
- IUPAC. (2013). "IUPAC Task Group on Atmospheric Chemical Kinetic Data Evaluation, (<http://iupac.pole-ether.fr>)."
- Madronich S. (2006). Chemical evolution of gaseous air pollutants down-wind of tropical megacities: Mexico City case study. *Atmospheric Environment* 40, 6012-6018.
- Magneron I., Bossoutrot V., Mellouki A., Laverdet G., Le Bras G. (2003). The OH-initiated oxidation of hexylene glycol and diacetone alcohol. *Environmental Science and Technology* 37, 4170-4181.

- Matsunaga S. N., Kawamura K. (2000). Determination of α - and β -hydroxycarbonyls and dicarbonyls in snow and rain samples by GC-FID and GC-MS employing benzyl hydroxyl oxime derivatization. *Analytical Chemistry* 72, 4742-4746.
- Mellouki A., Le Bras G., Sidebottom H. (2003). Kinetics and Mechanisms of the Oxidation of Oxygenated Organic Compounds in the Gas Phase. *Chemical Reviews* 103, 5077-5096.
- Messaadia L., El Dib G., Ferhati A., Roth E., Chakir A. (2012). Gas phase UV absorption cross-sections for a series of hydroxycarbonyls. *Chemical Physics Letters* 529, 16-22.
- Messaadia L., El Dib G., Lendar M., Cazaunau M., Roth E., Ferhati A., Mellouki A., Chakir A. (2013). Gas-phase rate coefficients for the reaction of 3-hydroxy-2-butanone and 4-hydroxy-2-butanone with OH and Cl. *Atmospheric Environment* 77, 951-958.
- Moortgat G. K. (2001). Important photochemical processes in the atmosphere. *Pure Applied Chemistry* 73, 487-490.
- Orlando J. J., Tyndall G. S. (2012). Laboratory studies of organic peroxy radical chemistry: an overview with emphasis on recent issues of atmospheric significance. *Chemical Society Reviews* 41, 6294-6317.
- Orlando J. J., Tyndall G. S., Fracheboud J. M., Estupinan E. G., Haberkorn S., Zimmer A. (1999). The rate and mechanism of the gas -phase oxidation of hydroxyacetone. *Atmospheric Environment* 33, 1621-1629.
- Reisen F., Aschmann S. M., Atkinson R., Arey J. (2003). Hydroxyaldehyde products from hydroxyl radical reactions of *z*-3-hexen-1-ol and 2-methyl-3-buten-2-ol quantified by SPME and API-MS. *Environmental Science and Technology* 37, 4664-4671.
- Sander S. P., Abbatt J. P. D., Barker J. R., Burkholder J. B., Friedl R. R., Golden D. M., Huie R. E., Kolb C. E., Kurylo M. J., Moortgat G. K., Orkin V. L., Wine P. H. (2011). Chemical kinetics and photochemical data for use in atmospheric studies, Evaluation No. 17. Pasadena, Jet Propulsion Laboratory, <http://jpldataeval.jpl.nasa.gov>.
- Singh H., Chen Y., Staudt A., Jacob D., Blake D., Heikes B., Snow J. (2001). Evidence from the Pacific troposphere for large global sources of oxygenated organic compounds. *Nature* 410, 1078-1081.
- Sleiman C., El Dib G., Tabet A., Canosa A. (2013). Atmospheric degradation of 4-hydroxy-4-methyl-2-pentanone with OH in the gas phase at 297 K. *Energy Procedia* 36, 502-510.
- Spaulding R., Charles M. (2002). Comparison of methods for extraction, storage, and silylation of pentafluorobenzyl derivatives of carbonyl compounds and multifunctional carbonyl compounds. *Analytical and Bioanalytical Chemistry* 372, 808-816.
- Szabo E., Djehiche M., Riva M., Fittschen C., Coddeville P., Sarzynski D., Tomas A., Dobé S. (2011). Atmospheric chemistry of 2,3-pentanedione: Photolysis and reaction with OH radicals. *Journal of Physical Chemistry A* 115, 9160-9168.
- Szabo E., Tarmoul J., Tomas A., Fittschen C., Dobe S., Coddeville P. (2009). Kinetics of the OH-radical initiated reactions of acetic acid and its deuterated isotopes. *Reaction Kinetics and Catalysis Letters* 96, 299-309.
- Téton S., Mellouki A., Le Bras G., Sidebottom H. (1996). Rate constants for reactions of OH radicals with a series of asymmetrical ethers and tert-butyl alcohol. *International Journal of Chemical Kinetics* 28, 291-297.

- 635 Tomas A., Villenave E., Lesclaux R. (2001). Reactions of the HO₂ radical with
636 CH₃CHO and CH₃C(O)O₂ in the gas phase. *Journal of Physical Chemistry A*
637 105, 3505-3514.
- 638 Tuazon E. C., Aschmann S. M., Arey J., Atkinson R. (1998). Products of the gas-
639 phase reactions of a series of methyl-substituted ethenes with the OH radical.
640 *Environmental Science and Technology* 32, 2106-2112.
- 641 Turpin E., Tomas A., Fittschen C., Devolder P., Galloo J.-C. (2006). Acetone-h₆ or -d₆
642 + OH reaction products: Evidence for heterogeneous formation of acetic acid
643 in a simulation chamber. *Environmental Science and Technology* 40, 5956-
644 5961.
- 645
646
647

Tables and Figures

Table 1: Experimental conditions used for the reaction of 3H3M2B with OH radicals in the Pyrex simulation chamber coupled to a FTIR spectrometer.

	3H3M2B + OH → products
Temperature (K)	298-356
Pressure (Torr)	500-600
Reference compound	Tert-butyl alcohol
Optical path (m)	24-56
[3H3M2B] ₀ (ppm)	10-50
[Reference] ₀ (ppm)	10-50
Spectral range (cm ⁻¹): 3H3M2B	990-950 and 3530-3480
Spectral range (cm ⁻¹): reference	1060-1000 and 3665-3620

Table 2: Photolysis frequencies, global quantum yields and product yields (corrected for wall loss and photolysis) of the photolysis of 3H3M2B in the absence and presence of OH-scavenger. Errors represent the global uncertainty (2 σ).

Experiments		
	Without OH-scavenger	With OH-scavenger
[3M3H2B] ₀ (ppm)	18 - 60	9 - 52
J _{3H3M2B} (h ⁻¹)	0.33 ± 0.02	0.24 ± 0.02
Φ _{3H3M2B} (270-390 nm)	-	0.79 ± 0.30
Molar yields of primary products (%)		
Acetone	86 ± 13	98 ± 14
Formaldehyde	16 ± 4	23 ± 4
Methanol	6 ± 1	11 ± 3 ^a 6 ± 1 ^b
2,3-butanedione	1.7 ± 0.5	0.4 ± 0.14
Methylglyoxal ^c	0.11 ± 0.05	0
Hydroxyacetone	NQ ^d	NQ ^d

^a: OH-scavenger: m-xylene

^b: OH-scavenger: carbon monoxide

^c: yield without photolysis correction

^d: NQ: not quantified

Table 3: Average rate constants for the reactions of 3H3M2B with OH

Temperature (K)	k_{3H3M2B}/k_{ref}	$k_{3H3M2B} (/ 10^{-13} \text{ cm}^3 \text{ molecule}^{-1} \text{ s}^{-1})$
298	0.67 ± 0.01	7.3 ± 1.0
298	0.69 ± 0.01	7.4 ± 1.0
298	0.75 ± 0.02	8.1 ± 1.0
		$7.6 \pm 0.5^*$
314	0.81 ± 0.01	9.2 ± 2.0
315	0.78 ± 0.01	8.9 ± 2.0
		$9.0 \pm 0.3^*$
334	0.81 ± 0.01	9.6 ± 1.5
334	0.75 ± 0.02	8.9 ± 1.5
335	0.76 ± 0.02	9.0 ± 1.5
		$9.2 \pm 0.4^*$
353	0.97 ± 0.01	12.0 ± 2.0
356	0.73 ± 0.02	9.2 ± 2.0
		$10.6 \pm 2.0^*$

* uncertainties correspond to the standard deviation of the rate constant

Figure 1: Kinetic plots of 3H3M2B photolysis. Empty symbols are for experiments without OH-scavenger (3 experiments), while full symbols are for experiments with excess m-xylene as OH-scavenger (2 experiments).

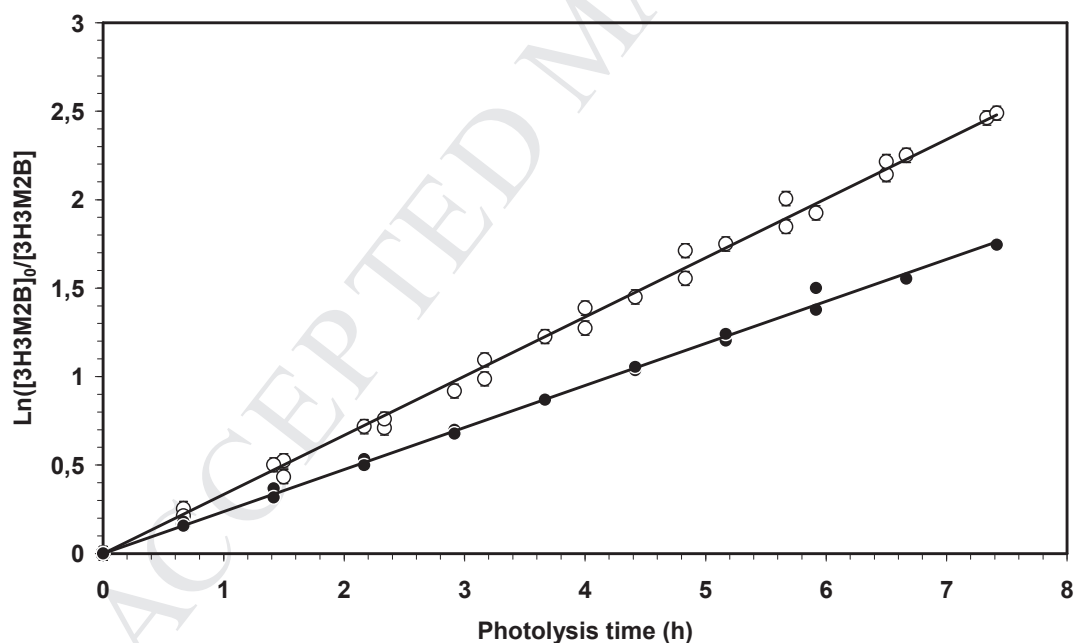


Figure 2: Time profiles of 3H3M2B and reaction products (experiment with m-xylene as OH-scavenger). Symbols: ○: 3H3M2B; △: Acetone; ◇: Acetic acid; *: Formaldehyde; ▽: Carbon monoxide; ◇: Methanol. Lines correspond to polynomial fits (except an exponential fit for 3H3M2B).

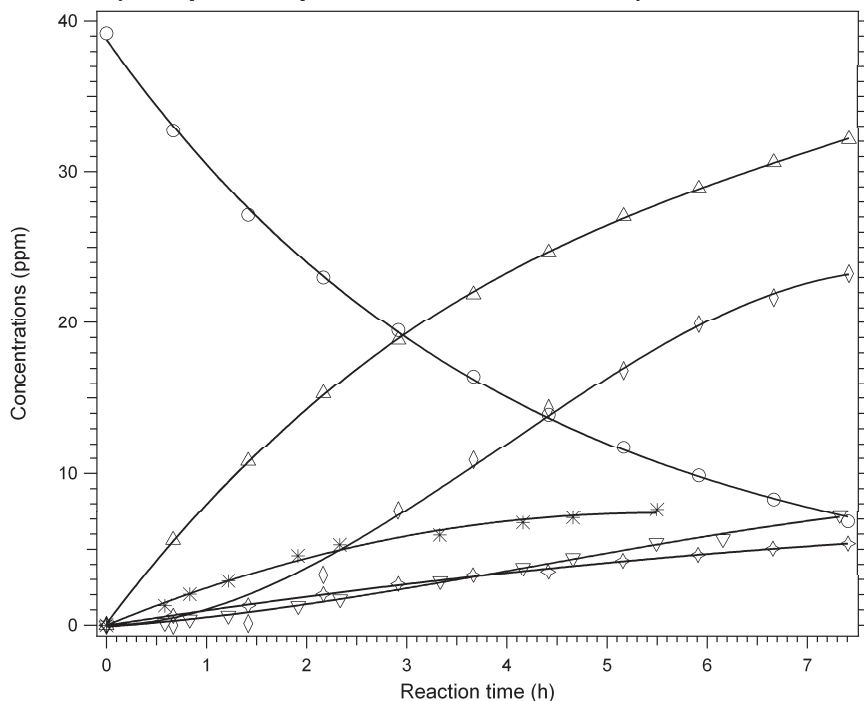


Figure 3: △: Acetone, *: Formaldehyde and ◇: Methanol yield plots for experiments performed in the presence of m-xylene as OH-scavenger. Lines correspond to linear fits for acetone and formaldehyde and to a polynomial fit (second order) for methanol.

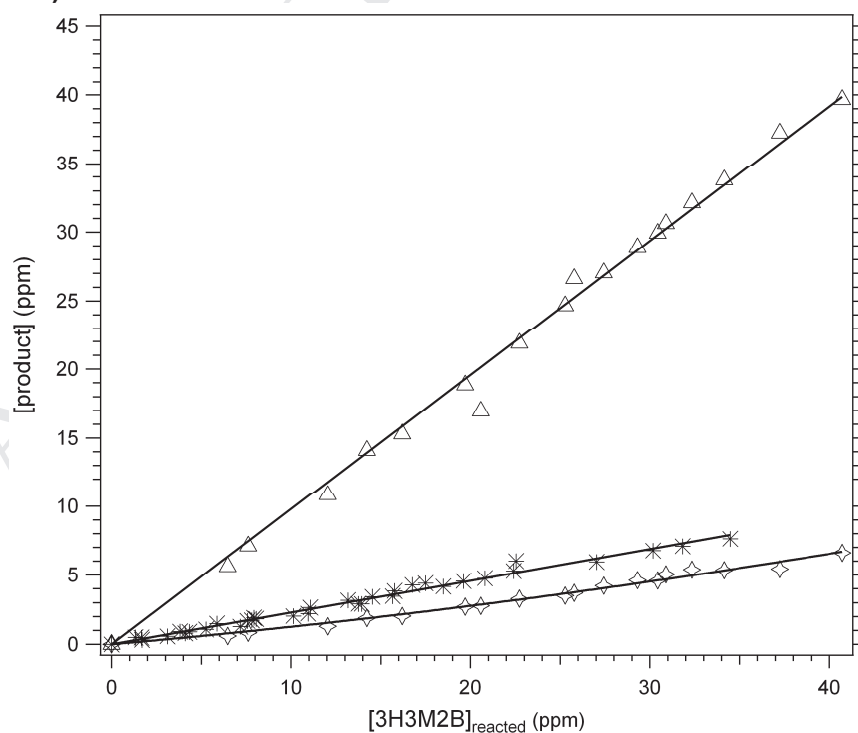


Figure 4: Plots of acetic acid (diamonds - left scale) and carbon monoxide (triangles - right scale) formation against 3H3M2B reacted. Full symbols are for experiments without OH-scavenger, while empty symbols are for experiments with OH-scavenger. Full lines correspond to polynomial fits of the data to help visualizing the data points.

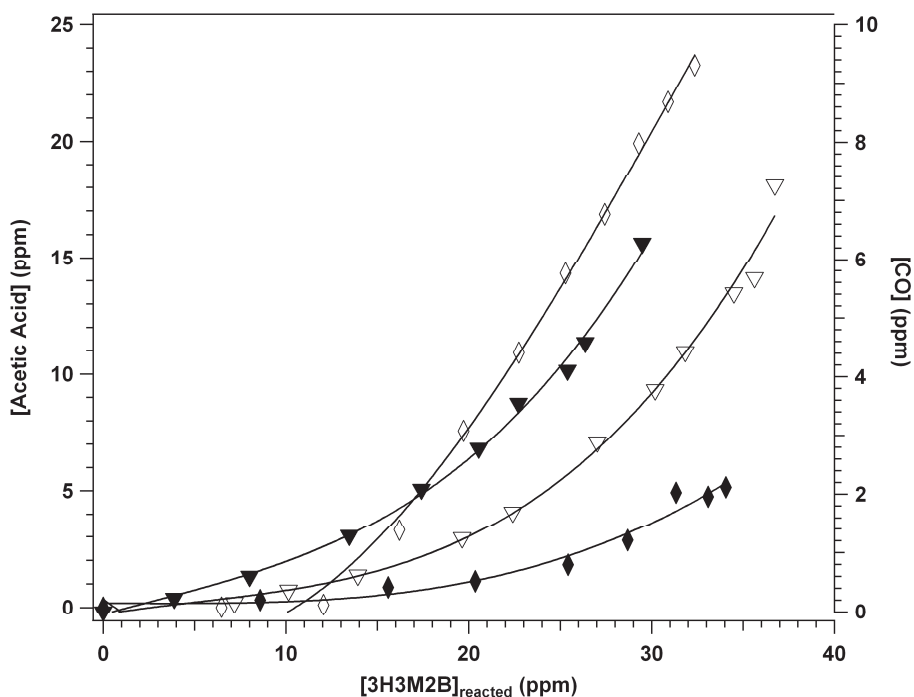


Figure 5: Simplified reaction mechanism for the photolysis of 3H3M2B

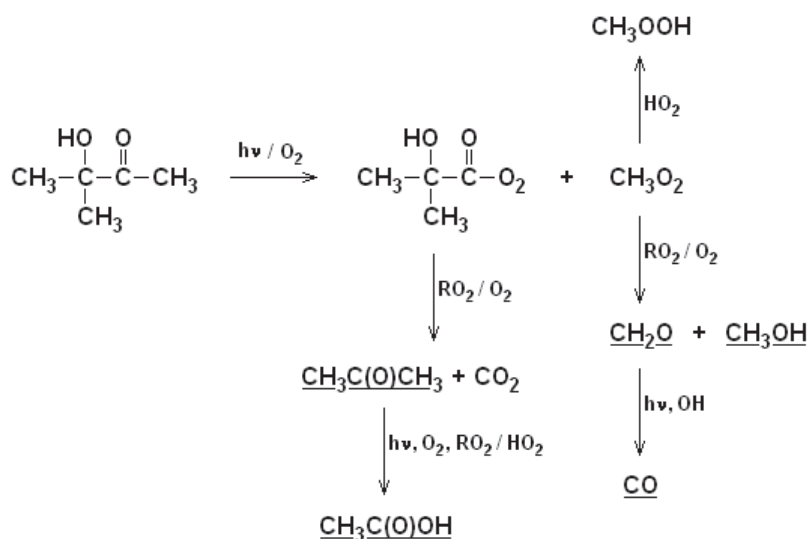


Figure 6: Relative rate plots for the reaction of OH with 3H3M2B according to eq. (VI) at different temperatures

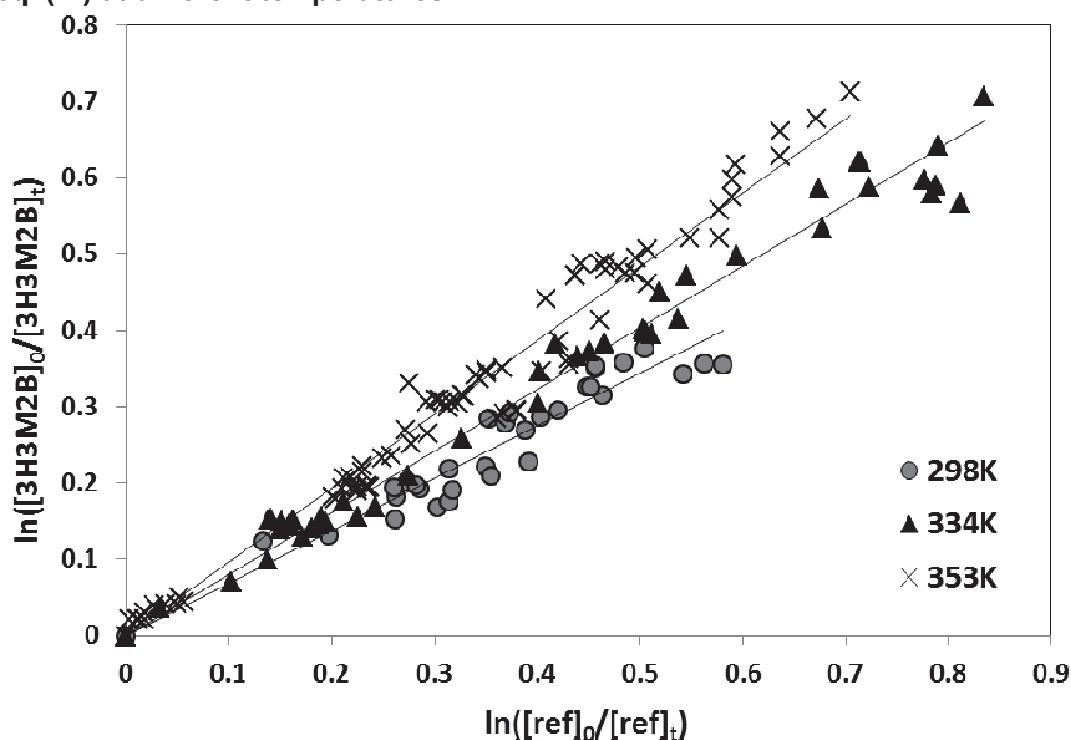
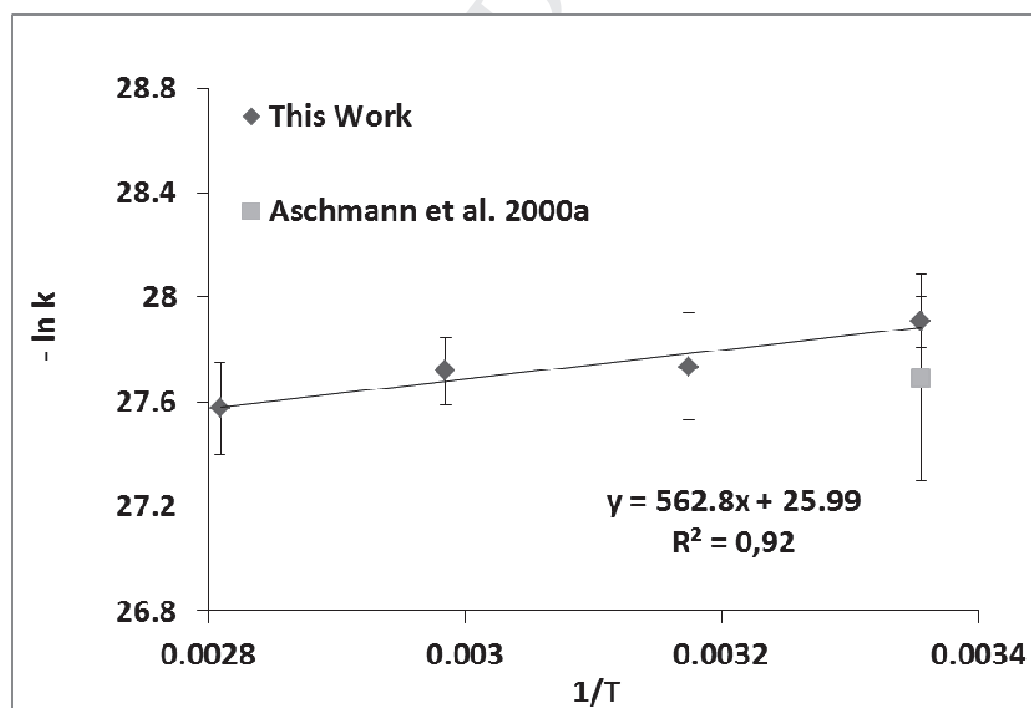


Figure 7: Arrhenius plot for the OH + 3H3M2B reaction between 298 and 356 K



Reactivity of 3-hydroxy-3-methyl-2-butanone: Photolysis and OH reaction kinetics

H. Bouzidi¹, H. Laversin², A. Tomas^{1*}, P. Coddeville¹, C. Fittschen³, G. El Dib⁴, E. Roth², A. Chakir²

¹Mines Douai, Département S.A.G.E, 59508 Douai, France

²Groupe de Spectrométrie Moléculaire et Atmosphérique, UMR CNRS 7331, Université de Reims, 51687 Reims, France

³Physico-chimie des Processus de Combustion et de l'Atmosphère, UMR CNRS 8522, Université Lille 1, 59655 Villeneuve d'Ascq, France

⁴Institut de Physique, Département de Physique Moléculaire, UMR 6251 CNRS, 35042 Rennes, France

* Corresponding author:

Alexandre TOMAS, alexandre.tomas@mines-douai.fr

Tel.: 33 327 712 651

Fax: 33 327 712 914

Highlights

- 3H3M2B photolysis is the major oxidation channel in the atmosphere
- Slight positive temperature dependence in the OH + 3H3M2B reaction kinetics
- Need for a better understanding of the atmospheric chemistry of oxygenated VOC